Title: Late Paleoproterozoic mafic magmatism and the Kalahari craton during Columbia assembly

Author: Cedric Djeutchou, Michiel O. de Kock, Hervé Wabo, Camilo E. Gaitán, Ulf Söderlund, Ashley P. Gumsley

Citation style: Djeutchou Cedric, de Kock Michiel O., Wabo Hervé, Gaitán Camilo E., Söderlund Ulf,. Gumsley Ashley P. (2021). Late Paleoproterozoic mafic magmatism and the Kalahari craton during Columbia assembly. „Geology (Boulder)" (2021, iss. 11, s. 1375-1380), DOI:10.1130/G48811.1

GEOLOGY | THE GEOLOGICAL SOCIETY OF AMERICA®

https://doi.org/10.1130/G48811.1

Manuscript received 11 January 2021
Revised manuscript received 17 May 2021
Manuscript accepted 24 May 2021

Late Paleoproterozoic mafic magmatism and the Kalahari craton during Columbia assembly

Cedric Djeutchou[1]*, Michiel O. de Kock[1], Hervé Wabo[1], Camilo E. Gaitán[2], Ulf Söderlund[2] and Ashley P. Gumsley[3]
[1]Department of Geology, University of Johannesburg, PO Box 524, Auckland Park 2006, South Africa
[2]Department of Geology, Lund University, Lund 223 62, Sweden
[3]Institute of Earth Sciences, University of Silesia in Katowice, Sosnowiec 41-200, Poland

ABSTRACT

The 1.87–1.84 Ga Black Hills dike swarm of the Kalahari craton (South Africa) is coeval with several regional magmatic provinces used here to resolve the craton's position during Columbia assembly. We report a new 1850 ± 4 Ma (U-Pb isotope dilution–thermal ionization mass spectrometry [ID-TIMS] on baddeleyite) crystallization age for one dike and new paleomagnetic data for 34 dikes of which 8 have precise U-Pb ages. Results are constrained by positive baked-contact and reversal tests, which combined with existing data produce a 1.87–1.84 Ga mean pole from 63 individual dikes. By integrating paleomagnetic and geochronological data sets, we calculate poles for three magmatic episodes and produce a magnetostratigraphic record. At 1.88 Ga, the Kalahari craton is reconstructed next to the Superior craton so that their ca. 2.0 Ga poles align. As such, magmatism forms part of a radiating pattern with the coeval ca. 1.88 Ga Circum-Superior large igneous province.

INTRODUCTION

The Paleoproterozoic to Mesoproterozoic supercontinent (referred to as Nuna, Hudsonland, or Columbia) formed by assembly of Archean cratons starting at 1.9 Ga and was fully amalgamated as late as 1.65–1.58 Ga (Meert, 2012; Pisarevsky et al., 2014; Pourteau et al., 2018). The position of the Kalahari craton (i.e., here the pre–1.2 Ga conjoined Kaapvaal and Zimbabwe cratons, or the proto-Kalahari craton, *sensu stricto*; see de Kock et al., 2021) in Columbia is obscured by limited paleomagnetic data. It does not appear in some reconstructions (e.g., Evans and Mitchell, 2011; Pehrsson et al., 2016), but in other reconstructions it is placed at Columbia's periphery (e.g., Zhao et al., 2003) or is regarded as a "lone craton" (Pisarevsky et al., 2014). A craton's position in Columbia is typically evaluated through 1.8–1.3 Ga apparent polar wander path comparison (Evans and Mitchell, 2011). For the Kalahari craton (simply Kalahari hereafter), post–1.8 Ga paleomagnetic data remain sparse (de Kock et al., 2021) and its tenure in Columbia remains unconstrained. Paleomagnetic data from 1.89 to 1.83 Ga magmatic provinces, however, can provide constraints on Kalahari's role in Columbia's assembly.

The current 1.89–1.83 Ga paleomagnetic record of Kalahari can be enhanced by studying its magmatic provinces (Fig. 1). The 1.87–1.84 Ga northeast- to north-northeast–trending mafic Black Hills dike swarm (BHDS; South Africa) is one such province (Olsson et al., 2016; Wabo et al., 2019). We present new paleomagnetic data from 36 BHDS dikes together with existing data from the 1.89–1.87 Ga Mashonaland sill province (Söderlund et al., 2010; Hanson et al., 2011) and the 1.88–1.87 Ga post-Waterberg sill province (Hanson et al., 2004). The BHDS is spatially, geochemically, and temporally associated with <1.83 Ga Soutpansberg Basin magmatism (Geng et al., 2014; Olsson et al., 2016) and the ca. 1.8 Ga Mazowe dike swarm of Zimbabwe (Fig. 1B) (Hanson et al., 2011). Paleomagnetic data from the Mashonaland and post-Waterberg sill provinces differ significantly and require large tectonic displacement between the Kaapvaal and Zimbabwe cratons (Hanson et al., 2011). Currently there is no geological support for such displacement. Another explanation may be rapid true polar wander (TPW) (Mitchell et al., 2010; Antonio et al., 2017). Unfortunately, few precisely dated Mashonaland intrusions also have paleomagnetic constraints (Table S3 in the Supplemental Material[1]). Furthermore, the BHDS was emplaced in the immediate aftermath of the proposed TPW. This limits careful evaluation of the discrepancy. Our data, however, provide a high-resolution paleomagnetic record to test Kalahari's 1.87–1.84 Ga paleogeography.

THE BLACK HILLS DIKE SWARM

The BHDS is a >300-km-wide swarm of mainly northeast- to north-northeast–trending mafic dikes intruding Archean basement, the 2.68–2.06 Ga Transvaal Supergroup, and the 2.06–2.05 Ga Bushveld and Phalaborwa Complexes (Olsson et al., 2016; Fig. 1). Paleoproterozoic magnetizations that pass reversal and baked-contact tests were reported for the BHDS (Letts et al., 2005, 2011; Lubnina et al., 2010) and are confirmed by combined U-Pb geochronology, geochemistry, and paleomagnetic data sets (Olsson et al., 2016; Wabo et al., 2019). Baddeleyite U-Pb crystallization ages of 12 dikes range between ca. 1.87 and ca. 1.84 Ga (Olsson et al., 2016; Wabo et al., 2019). However, only two dated dikes were also studied paleomagnetically (Lubnina et al., 2010; Wabo et al., 2019). Dike ages do not discriminate between trend or location but subdivide the swarm into an older, 1.88–1.86 Ga, more-primitive group and a younger, 1.85–1.84 Ga, more chemically enriched group (Olsson et al., 2016). The combined BHDS, Mashonaland, and Post-Waterberg sill provinces, and Soutpansberg Basin magmatism (Klausen et al., 2010; Lubnina et al., 2010; Olsson et al., 2016) form an ~50 m.y. record.

---

*E-mail: djeutchoucdric@yahoo.fr

[1]Supplemental Material. Geochronology, geochemistry, and paleomagnetic datasets. Please visit https://doi.org/10.1130/GEOL.S.14925186 to access the supplemental material, and contact editing@geosociety.org with any questions.

CITATION: Djeutchou, C., et al., 2021, Late Paleoproterozoic mafic magmatism and the Kalahari craton during Columbia assembly: Geology, v. 49, p. 1375–1380, https://doi.org/10.1130/G48811.1

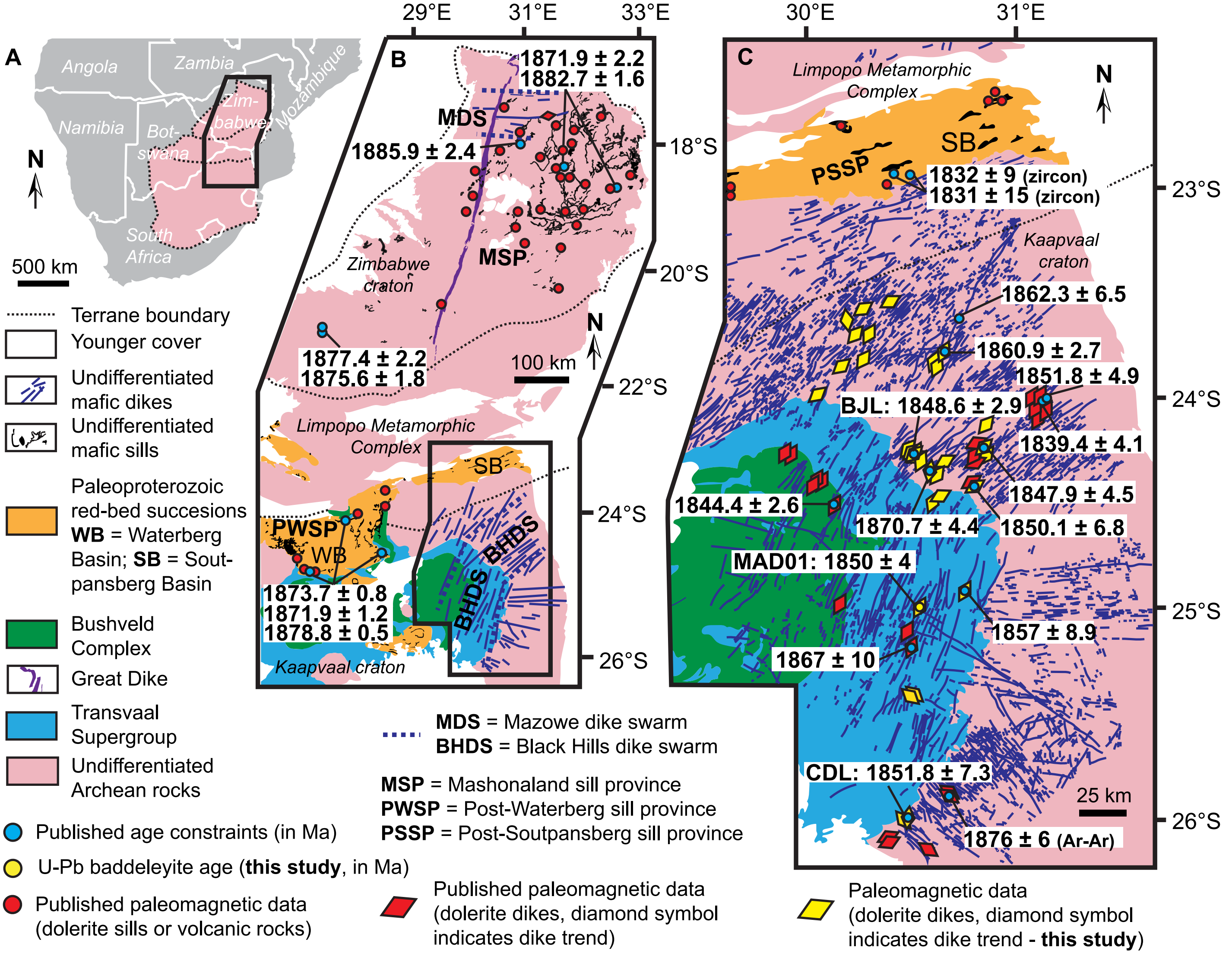

Figure 1. Simplified geological maps showing outlines of the Kalahari craton (A), pre–1.8 Ga Kalahari craton (B), and northeastern Kaapvaal craton (C) (adapted from de Kock et al., 2019; Hanson et al., 2011; Olsson et al., 2016). U-Pb baddeleyite age constraints are from the Mashonaland sill province (MSP; Söderlund et al., 2010; Hanson et al., 2011), post-Waterberg sill province (PWSP; Hanson et al., 2004); and Black Hills dike swarm (BHDS; Olsson et al., 2016; Wabo et al., 2019; this study). ^{40}Ar-^{39}Ar age is from Layer et al. (1998). Soutpansberg Basin U-Pb zircon ages are from Geng et al. (2014). Paleomagnetic data are from the MSP (McElhinny and Opdyke, 1964; Bates and Jones, 1996), Mazowe dike swarm (MDS; Wilson et al., 1987), PWSP (Hanson et al., 2004), BHDS (Layer et al., 1998; Lubnina et al., 2010; Letts et al., 2011; Maré and Fourie, 2012; Wabo et al., 2019; this study); and Soutpansberg Group and post-Soutpansberg sill province (PSSP; Hanson et al., 2004; Gose et al., 2006).

RESULTS

Geochronology

Baddeleyite grains extracted from an 8–10-m-thick north-northeast–trending dike (dike MAD01 in Fig. 1C) were divided into three fractions and dated by isotope dilution–thermal ionization mass spectrometry (ID-TIMS) at the Department of Geosciences, Swedish Museum of Natural History in Stockholm. The full methodology and data, including geochemistry (Table S2), are provided in the Supplemental Material. Free regression yields upper and lower intercepts at 1850 ± 4 Ma and 200 ± 250 Ma (mean squared weighted deviation [MSWD] = 1.13), respectively (Table S1; Fig. S1). The upper intercept is interpreted as the dike's crystallization age.

Paleomagnetism

We sampled 61 dikes for paleomagnetic study using standard methods (see the Supplemental Material; Table S3). Directly dated dikes were explicitly targeted. Each paleomagnetic site sampled a distinct dike and corresponds to a unique cooling unit. High-temperature magnetizations identified in 36 dikes are interpreted as Paleoproterozoic (Fig. 1; Fig. S2). The remaining 25 dikes had heterogeneous demagnetization behavior and are not discussed here (for more detail, see the Supplemental Material). High-temperature remanence components are grouped as northwest (downward) or southeast (upward), showing moderate to steep inclinations. Site means with radii of 95% confidence (α_{95}) >16° were excluded (i.e., 2 of our 36 dikes). The northwest and southeast groups share common precision and are ~180° apart, illustrating a class-C reversal test (Fig. S6). Sampling thus spans one or more reversals of the geomagnetic field. Two dated ca. 1.85 Ga dikes (Olsson et al., 2016), one north trending and one northeast trending (dikes CDL and BJL in Fig. 1C), have positive baked-contact tests supporting the primary Paleoproterozoic nature of the magnetization (see the Supplemental Material). Where directly dated, the crystallization age is assumed also to be the timing of remanence acquisition.

DISCUSSION

The 1.89–1.83 Ga Paleomagnetic Record

Paleomagnetic Data by Magmatic Province

Our data (34 dikes) are combined with published BHDS results (29 dikes; Table S3) to define two polarities (Fig. 2A; see the

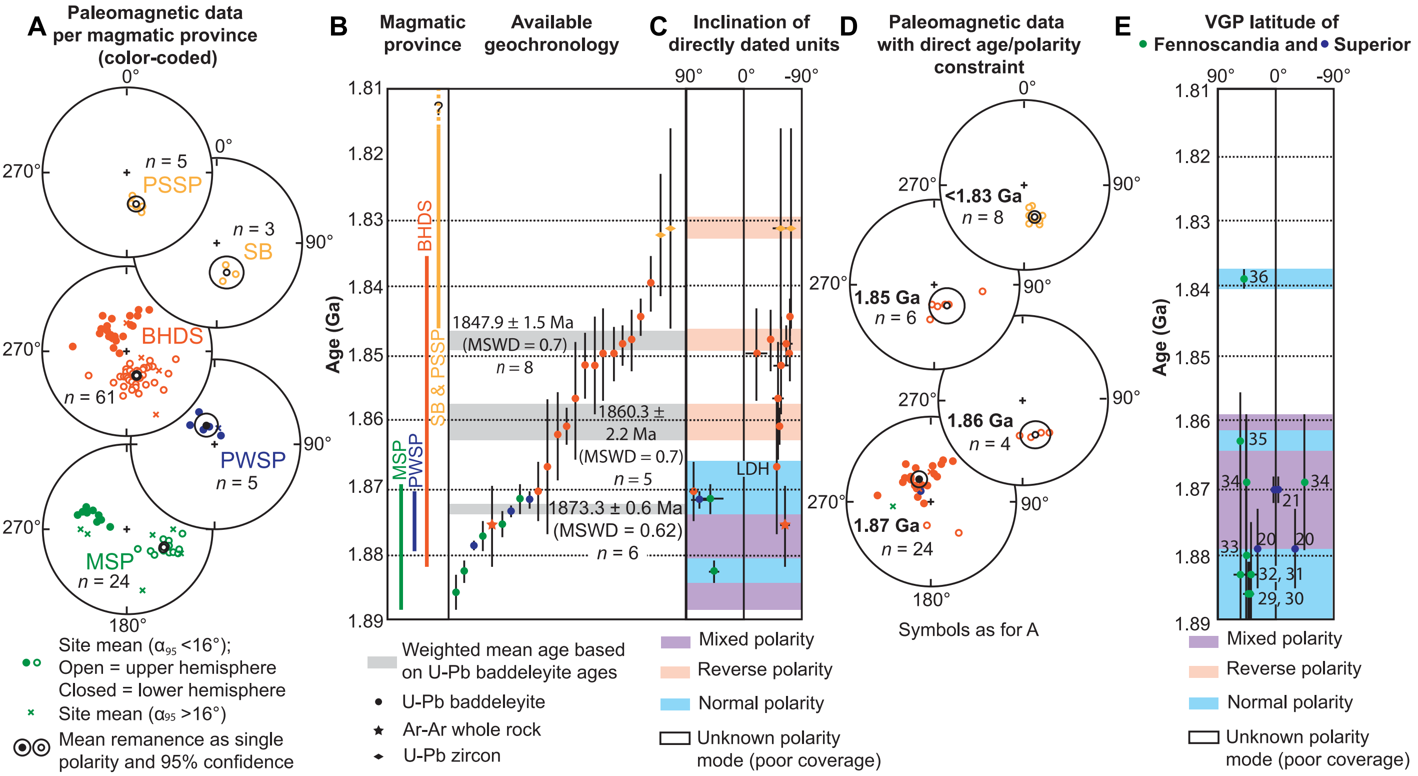

Figure 2. (A) Paleomagnetic site means from ca. 1.89 to <1.83 Ga units grouped and color coded according to magmatic province. The Post-Waterberg sill province (PWSP) mean differs significantly from the Mashonaland sill province (MSP) mean (the separation angle y0 = 25.4° > the critical angle $y_c = 11.0°$) but is indistinguishable from the Black Hills dike swarm (BHDS) mean ($y_0 = 4.9° < y_c = 14.1°$) and Soutpansberg Basin (SB) mean ($y_0 = 4.6° < y_c = 18.1°$). PSSP—post-Soutpansberg sill province. α_{95} is the radius of 95% confidence around the mean. (B) Crystallization ages and definition of magmatic episodes. (C) Magnetic inclination of directly dated units with dike LDH highlighted. MSWD—mean squared weighted deviation. Vertical error bars represent 2σ uncertainty in Ma, and horizontal error bars represent 95% confidence bounds of the inclination. (D) Site means according to age. BHDS dikes with positive inclination are inferred to belong to the ca. 1.87 Ga episode. The ca. 1.87 Ga mean is indistinguishable from the ca. 1.86 Ga mean ($y_0 = 11.9° < y_c = 20.3°$) and ca. 1.85 Ga mean ($y_0 = 1.4° < y_c = 15.9°$). (E) Fennoscandia and Superior virtual geomagnetic pole (VGP) latitude (numbering as per Table S4 [see footnote 1]).

Supplemental Material) and a mean paleopole for the BHDS at 15.3°N, 14.9°E and A_{95} (radii of 95% confidence) = 5.6° (Table S4; quality, Q, = 7; after Van der Voo, 1990). This pole represents ~30 m.y. and is indistinguishable from the 1.88–1.87 Ga Post-Waterberg sill province and <1.83 Ga Soutpansberg Basin poles (Table S4).

Magmatic Episodes and Magnetostratigraphy

Some units from regional magmatic provinces are coeval, and we calculated weighted mean crystallization ages (from U-Pb ID-TIMS baddeleyite dates; Fig. 2B) at 1873 ± 1 Ma (MSWD = 0.62), 1860 ± 2 Ma (MSWD = 0.7), and 1848 ± 2 Ma (MSWD = 0.7). These episodes refine the groupings of Olsson et al. (2016), who named the 1860 Ma episode as “old” and the ca. 1848 Ma episode as “young” BHDS. The crystallization age uncertainty of dike LDH of Wabo et al. (2019) allows it to be a member of either the 1873 Ma or 1860 Ma episode. Dike CDU of this study (sample BCD5-85 of Olsson et al., 2016) can similarly be a member of either the 1860 Ma or 1848 Ma episode. Units of the ca. 1873 Ma episode all have positive inclinations (Fig. 2C). Negatively inclined dike LDH thus likely belongs to the ca. 1860 Ma episode, which is exclusively represented by dikes of negative inclination (Fig. 2C). Besides polarity, the chemical composition provides another discriminator between episodes (Olsson et al., 2016). We note that dikes MAD01 (herein dated at 1850 ± 5 Ma) and LDH (dated at 1867 ± 10 Ma by Wabo et al. [2019]) have MgO contents of 4.9 wt% and 6.0 wt%, respectively (Table S2), which are comparable to those of the “young” and “old” groups, respectively.

Only two paleomagnetically constrained units of the Mashonaland sill province are directly dated. One sill has an age corresponding to the ca. 1873 Ma episode, and it has a positive inclination as expected. An older ca. 1883 Ma sill also has positive inclination. The Mashonaland data thus span at least two reversals, and mixed polarity is otherwise assigned to the province (Fig. 2C).

Mean poles are calculated for episodes based on dated units. Such poles are temporally better defined than magmatic province poles (Fig. 2D; Table S4). Dated BHDS dikes were exclusively of negative inclination during the ca 1860 Ma and ca. 1848 Ma episodes and of positive inclination during the ca. 1873 Ma episode (Fig. 2C). This defines a late Paleoproterozoic magnetostratigraphic record for Kalahari. All undated BHDS dikes that recorded positive inclinations were used to calculate a ca. 1873 Ma episode pole (11.8°N, 10.6°E and A_{95} = 11.8°; Table S4; Q = 7). Poles at ca. 1860 Ma and ca. 1848 Ma have larger uncertainties but are statistically indistinguishable from the ca. 1873 Ma pole (Table S4).

Kalahari and Columbia’s Assembly

The timing of Columbia’s assembly and its final configuration is debated (Meert, 2012), but there is consensus that Baltica, Laurentia, and Siberia formed the core around which other continents were accreted (e.g., Evans and Mitchell, 2011; Pehrsson et al., 2016), while the suture between Laurentia and Australia occurred as late as 1.6 Ga (Pourteau et al., 2018). At 1.88 Ga, Baltica and Laurentia were not fully assembled. Sarmatia and Volgo-Uralia collided with Fennoscandia (i.e., the Kola craton, Karelia craton, and Svecofennian crust) at 1.82–1.80 Ga to form Baltica. Overlap of 1.89–1.79 Ga Fennoscandian poles suggests that it was fairly stationary (Klein et al., 2016; Fig. 3D). Laurentian

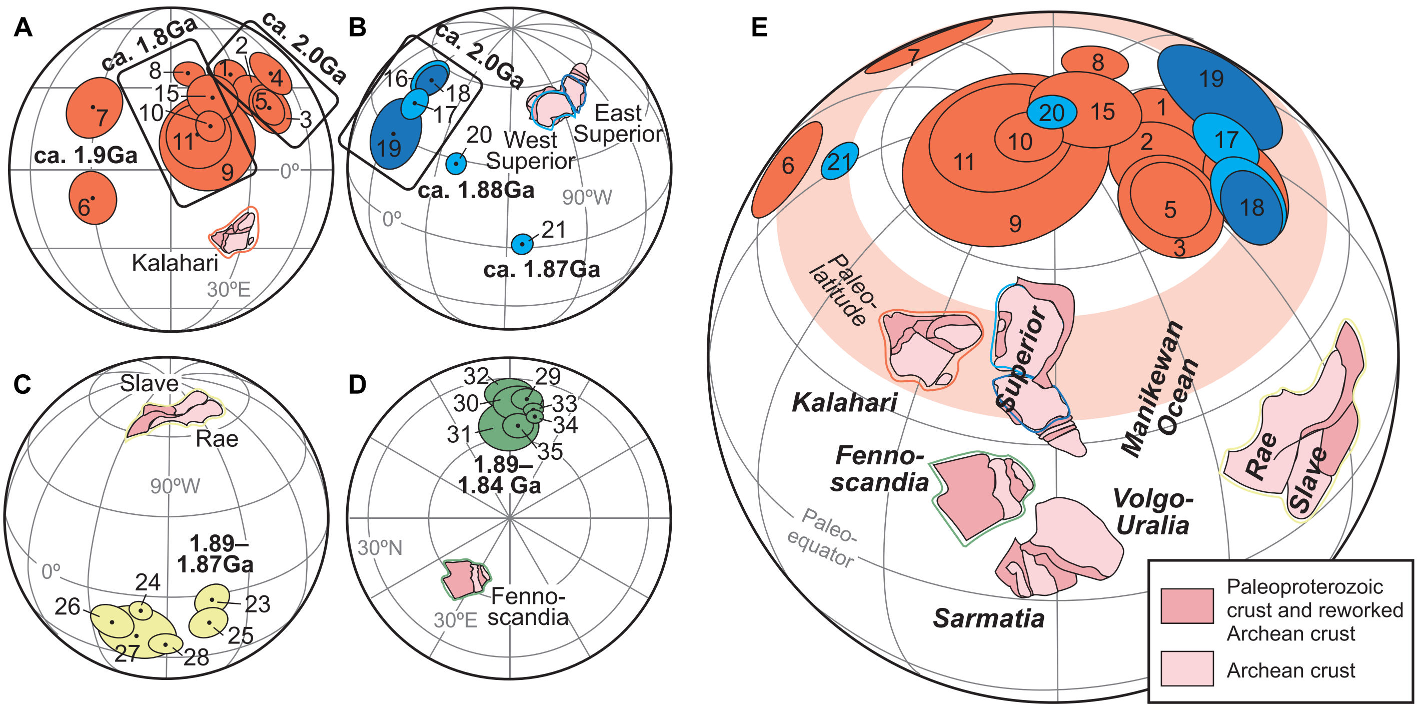

Figure 3. (A,B) The ca. 2.0–1.8 Ga paleopoles for the Kalahari (A) and Superior (corrected for relative rotation) (B) cratons. The West Superior craton and its poles are shown in light blue, and the East Superior craton and its poles are shown in dark blue. (C) The Slave craton 1.89–1.87 Ga paleopoles. (D) The Fennoscandia 1.89–1.84 Ga paleopoles. (E) Reconstruction at 1.88 Ga. Kalahari's band of allowed paleolatitudinal reconstructions is shown. All poles are numbered as per Table S4 (see footnote 1).

assembly occurred between ca. 1.91 Ga and 1.81 Ga (e.g., Mitchell et al., 2014), and its data are discordant. For Superior poles, some discordance is resolved by straightening the Kapuskasing zone (Evans and Halls, 2010). For the Slave and Superior cratons (Figs. 3B and 3C), TPW may account for the remaining dispersion (Mitchell et al., 2010).

A comparison of absolute polarity can constrain the relative positions of the Superior, Fennoscandia, and Kalahari cratons. In the late Paleoproterozoic, absolute polarity is assigned to Laurentia based on trade-wind orographic patterns across the Slave craton (Hoffman and Grotzinger, 1993). Driscoll and Evans (2016) followed this rationale and assigned positive inclinations from the Superior craton as normal polarity. In this vane, Fennoscandia showed normal polarity before ca. 1.88 Ga (Fig. 2D). Normal polarity is constrained in Kalahari by a single dated Mashonaland sill. Mixed polarities between 1.89 Ga and 1.87 Ga are otherwise recorded by the Mashonaland sill province (Fig. 2C). Between ca. 1.88 Ga and ca. 1.86 Ga, dual magnetic polarities are described from the ca. 1870 ± 9 Ma Svecofennian Keuruu dikes (paleopole 34 in Table S4; Fig. 2D). The reversal(s) recorded by these dikes can be correlated to either the 1873 Ma or pre–1873 Ma reversals of Kalahari. Normal polarity is reported from the ca. 1863 ± 7 Ma Eastern Murmansk sills of the Kola craton (paleopole 35 in Table S4; Fig. 2D). Given current age constraints, this normal polarity cannot be separated from the ca. 1873 Ma normal polarity chron of Kalahari. The ca. 1840–1837 Ma Haukivesi intrusion (Svecofennia) provides an isolated normal polarity data point for Fennoscandia (paleopole 36 in Table S4; Fig. 2D), but there are no data to compare with Kalahari. On Kalahari, several sites from the <1.83 Ga Soutpansberg Basin yield reverse polarity (Fig. 2C). The shared normal polarity before ca. 1.88 Ga and shared record of a reversal at ca. 1.87 Ga suggest that Fennoscandia and Kalahari were in the same hemisphere, although this should be tested as new data become available.

On the Superior craton, the ca. 1.88 Ga Molson dikes record dual polarities as does the ca. 1.87 Ga Haig-Flaherty-Sutton mean (paleopoles 20 and 21 in Table S4; Fig. 2D). Reversals represented by these data may correlate to the post–1873 Ma Kalahari reversal. It is, however, important to note potential disagreement with this model in terms of 1850–1830 Ma normal polarities recorded by the ca. 1850 Ma but poorly dated Sudbury irruptive and the ca. 1838 Ma Boot-Phantom pluton (Hood, 1961; Symons and McKay, 1999). Both these results were, however, excluded from quality-filtered Laurentian data (Swanson-Hysell, 2021).

At 1.88 Ga, Kalahari restores to 45°–59° paleolatitude, Fennoscandia to 11°–28°, and the Superior craton to 32°–58° (Fig. 3E). The Superior-Nain block can be placed in a position northeast of Fennoscandia preceding the Northern Europe–North America (NENA) configuration (Klein et al., 2016) by overlapping the 1.88 Ga Molson dikes pole with 1.89–1.84 Ga Fennoscandian poles (Figs. 3B and 3D). The 1.89–1.83 Ga Kalahari poles are overlapped with the 1.88 Ga Molson dikes pole. Kalahari is placed to the west of the reconstructed Superior craton adjacent to the Penokean orogen (Fig. 3E). The modern southwestern margin of the Superior craton is occupied by the 1.77–1.60 Ga Central Plains, Yavapai, and Mazatzal orogens (Whitmeyer and Karlstrom, 2007). Placing Kalahari to the east of the Superior craton is permissible in paleolatitude, but the area is occupied by the Manikewan Ocean (Fig. 3E). Restoration of Kalahari to the west of the Superior craton, in contrast to "lone-craton" configurations, aligns the BHDS and the Mazowe dike swarm into a radiating pattern around the ca. 1.88 Ga Circum-Superior large igneous province magmatic center (Minifie et al., 2013). This event thus likely included the intraplate magmatism of Kalahari as well as that of Fennoscandia (Fig. 4). In this position, overlap is also achieved between the ca. 2.0 Ga Kalahari and Superior craton poles (Fig. 3E). This suggests a longer-lived link, and it is interesting to note that the Kaapvaal craton at ca. 2.43 Ga was similarly reconstructed (Gumsley et al., 2017). If this is correct, it implies that a loop in apparent polar wander (defined by paleopoles 6 and 7 in Table S4; Fig. 3A) has gone unrecognized in the Superior craton. Furthermore, in our model, there is alignment between the Kapuskasing zone of the Superior craton and the Thabazimbi-Murchison lineament

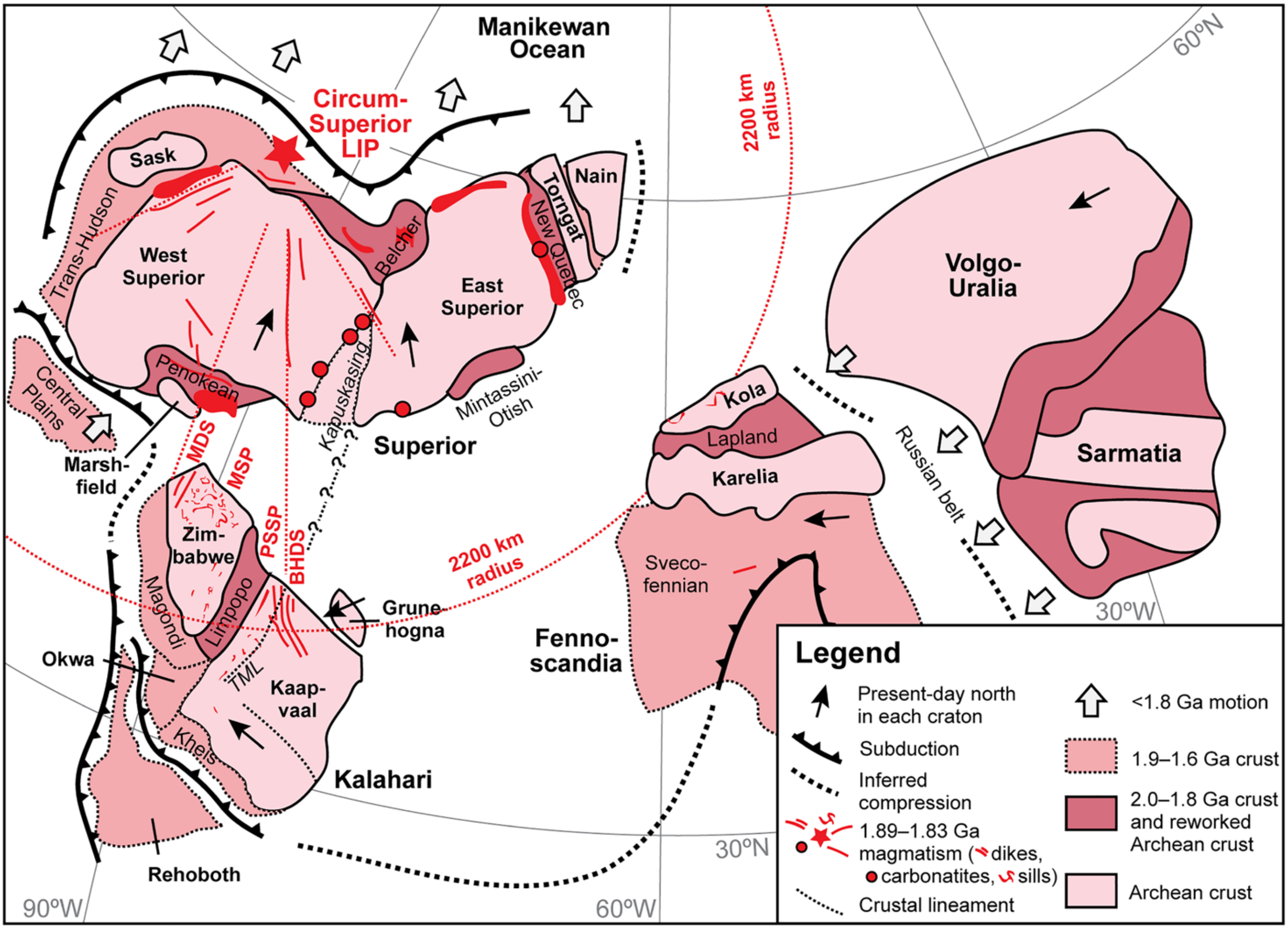

Figure 4. Reconstruction of the Kalahari craton at 1.88 Ga relative to the West Superior craton (Euler parameters as per Table S5 [see footnote 1]) revealing radiating pattern of 1.88–1.83 Ga magmatism around the Circum-Superior large igneous province (LIP) center (star). Pole numbering is as per Table S4. TML—Thabazimbi-Murchison lineament. Other abbreviations are as per Figure 1.

of Kalahari, as well as possible continuation between the Limpopo and Penokean orogens (Fig. 4). On the opposite side of the Manikewan Ocean, the Slave-Rae craton is reconstructed at low paleolatitude using the ca. 1.88 Ga Ghost dike swarm and mean Kahochella–Peacock Hills poles (paleopoles 23 and 25 in Table S4; Fig. 3C). The Ghost dike swarm pole is considered more reliable than similarly aged poles from the Slave craton (Swanson-Hysell, 2021).

After ca. 1.88 Ga, Kalahari and Fennoscandia remained fairly fixed as formation of the Russian belt concluded the assembly of Baltica. At the same time, the Superior craton is envisaged to have rotated clockwise into a classic NENA configuration, leading to possible extension between it and Kalahari and the ultimate closure of the Manikewan Ocean. Unfortunately, a 1.83–1.40 Ga lacuna in Kalahari's paleomagnetic data prevent evaluation of its position throughout the existence of Columbia, but our 1.88 Ga reconstruction does suggest a peripheral position for the craton early during Columbia's assembly.

ACKNOWLEDGMENTS

We thank D.A.D. Evans, R.N. Mitchell, and an anonymous reviewer. C. Djeutchou, M. de Kock and H. Wabo acknowledge support of the South African Department of Science and Innovation–National Research Foundation Centre of Excellence for Integrated Mineral and Energy Resource Analysis (DSI-NRF CIMERA) and a National Research Foundation development grant (RDYR14080787934). A. Gumsley acknowledges support through a Polish National Science Centre grant (POLONEZ grant UMO-2016/23/P/ST10/02423), funded from the European Union's Horizon 2020 research and innovation program under the Marie Skłodowska-Curie Actions CO-FUND-2014 (grant 665778). A. Gumsley also acknowledges the support of the EPOS-PL project (No. POIR.04.02.00-14-A003/16), co-financed by the European Union from funds of the European Regional Development Fund (ERDF) to the laboratory facilities at IG PAS used in the study.

REFERENCES CITED

Antonio, P.Y.J., D'Agrella-Filho, M.S., Trindade, R.I.F., Nédélec, A., de Oliveira, D.C., da Silva, F.F., Roverato, M., and Lana, C., 2017, Turmoil before the boring billion: Paleomagnetism of the 1880–1860 Ma Uatumã event in the Amazonian craton: Gondwana Research, v. 49, p. 106–129, https://doi.org/10.1016/j.gr.2017.05.006.

Bates, M.P., and Jones, D.L., 1996, A palaeomagnetic investigation of the Mashonaland dolerites, northeast Zimbabwe: Geophysical Journal International, v. 126, p. 513–524, https://doi.org/10.1111/j.1365-246X.1996.tb05307.x.

de Kock, M.O., Gumsley, A.P., Klausen, M.B., Söderlund, U., and Djeutchou, C., 2019, The Precambrian mafic magmatic record, including large igneous provinces of the Kalahari craton and its constituents: A paleogeographic review, *in* Srivastava, R.K., et al., eds., Dyke Swarms of the World: A Modern Perspective: Singapore, Springer, p. 155–214, https://doi.org/10.1007/978-981-13-1666-1_5.

de Kock, M.O., Luskin, C.R., Djeutchou, C., and Wabo, H., 2021, The Precambrian drift history and paleogeography of the Kalahari craton, *in* Pesonen, L.J., et al., eds., Ancient Supercontinents and the Paleogeography of the Earth: Amsterdam, Elsevier (in press).

Driscoll, P.E., and Evans, D.A.D., 2016, Frequency of Proterozoic geomagnetic superchrons: Earth and Planetary Science Letters, v. 437, p. 9–14, https://doi.org/10.1016/j.epsl.2015.12.035.

Evans, D.A.D., and Halls, H.C., 2010, Restoring Proterozoic deformation within the Superior craton: Precambrian Research, v. 183, p. 474–489, https://doi.org/10.1016/j.precamres.2010.02.007.

Evans, D.A.D., and Mitchell, R.N., 2011, Assembly and breakup of the core Paleo-Mesoproterozoic supercontinent Nuna: Geology, v. 39, p. 443–446, https://doi.org/10.1130/G31654.1.

Geng, H., Brandl, G., Sun, M., Wong, J., and Kröner, A., 2014, Zircon ages defining deposition of the Palaeoproterozoic Soutpansberg Group and further evidence for Eoarchaean crust in South Africa: Precambrian Research, v. 249, p. 247–262, https://doi.org/10.1016/j.precamres.2014.05.020.

Gose, W.A., Hanson, R.E., Dalziel, I.W.D., Pancake, J.A., and Seidel, E.K., 2006, Paleomagnetism of the 1.1 Ga Umkondo large igneous province in southern Africa: Journal of Geophysical Research, v. 111, B09101, https://doi.org/10.1029/2005JB003897.

Gumsley, A.P., Chamberlain, K.R., Bleeker, W., Söderlund, U., de Kock, M.O., Larsson, E.R., and Bekker, A., 2017, Timing and tempo of the Great Oxidation Event: Proceedings of the National Academy of Sciences of the United States of America, v. 114, p. 1811–1816, https://doi.org/10.1073/pnas.1608824114.

Hanson, R.E., Gose, W.A., Crowley, J.L., Ramezani, J., Bowring, S.A., Bullen, D.S., Hall, R.P., Pancake, J.A., and Mukwakwami, J., 2004, Paleoproterozoic intraplate magmatism and basin development on the Kaapvaal Craton: Age, paleomagnetism and geochemistry of ~1.93 to ~1.87 Ga post-Waterberg dolerites: South African Journal of Geology, v. 107, p. 233–254, https://doi.org/10.2113/107.1-2.233.

Hanson, R.E., Rioux, M., Gose, W.A., Blackburn, T.J., Bowring, S.A., Mukwakwami, J., and Jones, D.L., 2011, Paleomagnetic and geochronological evidence for large-scale post–1.88 Ga displacement between the Zimbabwe and Kaapvaal cratons along the Limpopo belt: Geology, v. 39, p. 487–490, https://doi.org/10.1130/G31698.1.

Hoffman, P.F., and Grotzinger, J.P., 1993, Orographic precipitation, erosional unloading, and tectonic style: Geology, v. 21, p. 195–198, https://doi.org/10.1130/0091-7613(1993)021<0195:OPEUAT>2.3.CO;2.

Hood, P.J., 1961, Paleomagnetic study of the Sudbury Basin: Journal of Geophysical Research, v. 66, p. 1235–1241, https://doi.org/10.1029/JZ066i004p01235.

Klausen, M.B., Söderlund, U., Olsson, J.R., Ernst, R.E., Armoogam, M., Mkhize, S.W., and Petzer, G., 2010, Petrological discrimination among Precambrian dyke swarms: Eastern Kaapvaal craton (South Africa): Precambrian Research, v. 183, p. 501–522, https://doi.org/10.1016/j.precamres.2010.01.013.

Klein, R., Pesonen, L.J., Mänttäri, I., and Heinonen, J.S., 2016, A late Paleoproterozoic key pole for the Fennoscandian Shield: A paleomagnetic study of the Keuruu diabase dykes, Central Finland: Precambrian Research, v. 286, p. 379–397, https://doi.org/10.1016/j.precamres.2016.10.013.

Layer, P.W., Lopez-Martinez, M., Kröner, A., York, D., and McWilliams, M., 1998, Thermochronology and paleomagnetism of the Archean Nelshoogte Pluton, South Africa: Geophysical Journal International, v. 135, p. 129–145, https://doi.org/10.1046/j.1365-246X.1998.00613.x.

Letts, S., Torsvik, T.H., Webb, S.J., Ashwal, L.D., Eide, E.A., and Chunnett, G., 2005, Palaeomagnetism and ^{40}Ar/^{39}Ar geochronology of mafic dykes from the eastern Bushveld Complex (South Africa): Geophysics Journal International, v. 162, p. 36–48, https://doi.org/10.1111/j.1365-246X.2005.02632.x.

Letts, S., Torsvik, T.H., Webb, S.J., and Ashwal, L.D., 2011, New Palaeoproterozoic paleomagnetic data from the Kaapvaal Craton, South Africa, *in* van Hinsbergen, D.J.J., et al., eds., The Formation and Evolution of Africa: A Synopsis of 3.8 Ga of Earth History: Geological Society [London] Special Publication 357, p. 9–26, https://doi.org/10.1144/SP357.2.

Lubnina, N., Ernst, R., Klausen, M., and Söderlund, U., 2010, Paleomagnetic study of Neoarchean–Paleoproterozoic dykes in the Kaapvaal Craton: Precambrian Research, v. 183, p. 523–552, https://doi.org/10.1016/j.precamres.2010.05.005.

Maré, L.P., and Fourie, C.J.S., 2012, New geochemical and palaeomagnetic results from Neoarchaean dyke swarms in the Badplaas-Barberton area, South Africa: South African Journal of Geology, v. 115, p. 145–170, https://doi.org/10.2113/gssajg.115.2.145.

McElhinny, M.W., and Opdyke, N.D., 1964, The paleomagnetism of the Precambrian dolerites of eastern Southern Rhodesia, an example of geologic correlation by rock magnetism: Journal of Geophysical Research, v. 69, p. 2465–2475, https://doi.org/10.1029/JZ069i012p02465.

Meert, J.G., 2012, What's in a name? The Columbia (Paleopangea/Nuna) supercontinent: Gondwana Research, v. 21, p. 987–993, https://doi.org/10.1016/j.gr.2011.12.002.

Minifie, M.J., Kerr, A.C., Ernst, R.E., Hastie, A.R., Ciborowski, T.J.R., Desharnais, G., and Millar, I.L., 2013, The northern and southern sections of the western ca. 1880 Ma Circum-Superior Large Igneous Province, North America: The Pickle Crow dyke connection?: Lithos, v. 174, p. 217–235, https://doi.org/10.1016/j.lithos.2012.03.017.

Mitchell, R.N., Hoffman, P.F., and Evans, D.A.D., 2010, Coronation loop resurrected: Oscillatory apparent polar wander of Orosirian (2.05–1.8 Ga) paleomagnetic poles from Slave craton: Precambrian Research, v. 179, p. 121–134, https://doi.org/10.1016/j.precamres.2010.02.018.

Mitchell, R.N., Bleeker, W., van Breemen, O., Lecheminant, T.N., Peng, P., Nilsson, M.K.M., and Evans, D.A.D., 2014, Plate tectonics before 2.0 Ga: Evidence from paleomagnetism of cratons within supercontinent Nuna: American Journal of Science, v. 314, p. 878–894, https://doi.org/10.2475/04.2014.03.

Olsson, J.R., Klausen, M.B., Hamilton, M.A., März, N., Söderlund, U., and Roberts, R.J., 2016, Baddeleyite U-Pb ages and geochemistry of the 1875–1835 Ma Black Hills Dyke Swarm across north-eastern South Africa: Part of a trans-Kalahari Craton back-arc setting?: GFF, v. 138, p. 183–202, https://doi.org/10.1080/11035897.2015.1103781.

Pehrsson, S.J., Eglington, B.M., Evans, D.A.D., Huston, D., and Reddy, S.M., 2016, Metallogeny and its link to orogenic style during the Nuna supercontinent cycle, *in* Li, Z.X., et al., eds., Supercontinent Cycles Through Earth History: Geological Society [London] Special Publication 424, p. 83–94, https://doi.org/10.1144/SP424.5.

Pisarevsky, S.A., Elming, S.-Å., Pesonen, L.J., and Li, Z.-X., 2014, Mesoproterozoic paleogeography: Supercontinents and beyond: Precambrian Research, v. 244, p. 207–225, https://doi.org/10.1016/j.precamres.2013.05.014.

Pourteau, A., Smit, M.A., Li, Z.-X., Collins, W.J., Nordsvan, A.R., Volante, S., and Li, J., 2018, 1.6 Ga crustal thickening along the final Nuna suture: Geology, v. 46, p. 959–962, https://doi.org/10.1130/G45198.1.

Söderlund, U., Hofmann, A., Klausen, M.B., Olsson, J.R., Ernst, R.E., and Persson, P.-O., 2010, Towards a complete magmatic barcode for the Zimbabwe craton: Baddeleyite U-Pb dating of regional dolerite dyke swarms and sill complexes: Precambrian Research, v. 183, p. 388–398, https://doi.org/10.1016/j.precamres.2009.11.001.

Swanson-Hysell, N.L., 2021, The Precambrian paleogeography of Laurentia, *in* Pesonen, L.J., et al., eds., Ancient Supercontinents and the Paleogeography of the Earth: Amsterdam, Elsevier (in press).

Symons, D.T.A., and McKay, C.P., 1999, Paleomagnetism of the Boot-Phantom pluton and the amalgamation of the juvenile domains in the Paleoproterozoic Trans-Hudson orogen, Canada, *in* Sinha, A.K., ed., Basement Tectonics 13: Proceedings of the Thirteenth International Conference on Basement Tectonics, held in Blacksburg, Virginia, U.S.A., June 1997: Dordrecht, Springer, p. 313–331, https://doi.org/10.1007/978-94-011-4800-9_18.

Van der Voo, R., 1990, The reliability of paleomagnetic data: Tectonophysics, v. 184, p. 1–9, https://doi.org/10.1016/0040-1951(90)90116-P.

Wabo, H., Humbert, F., de Kock, M.O., Söderlund, U., Maré, L., and Beukes, N.J., 2019, Constraining the chronology of the Mashishing dykes from the eastern Kaapvaal craton in South Africa, *in* Srivastava, R.K., et al., eds., Dyke Swarms of the World: A Modern Perspective: Singapore, Springer, https://doi.org/10.1007/978-981-13-1666-1_6.

Whitmeyer, S.J., and Karlstrom, K.E., 2007, Tectonic model for the Proterozoic growth of North America: Geosphere, v. 3, p. 220–259, https://doi.org/10.1130/GES00055.1.

Wilson, J.F., Jones, D.L., and Kramers, J.D., 1987, Mafic dyke swarms of Zimbabwe, *in* Halls, H.C., and Fahring, A.F., eds., Mafic Dyke Swarms: Geological Association of Canada Special Paper 34, p. 433–444.

Zhao, G., Sun, M., Wilde, S.A., and Li, S., 2003, Assembly, accretion and breakup of the Paleo-Mesoproterozoic Columbia Supercontinent: Records in the North China Craton: Gondwana Research, v. 6, p. 417–434, https://doi.org/10.1016/S1342-937X(05)70996-5.

Printed in USA